Natural Hazards (2024) 120:4875–4900
https://doi.org/10.1007/s11069-024-06401-x

ORIGINAL PAPER

Assessing tsunami risk along the Aceh coast, Indonesia: a quantitative analysis of fault rupture potential and early warning system efficacy for predicting arrival time and flood extent

Benazir[1] · **Rina Suryani Oktari**[2]

Received: 17 October 2023 / Accepted: 30 December 2023 / Published online: 30 January 2024

Abstract
The Aceh coast (western Indonesia) is prone to regular tsunamis, as evidenced by historical records and paleo-tsunami studies. Effective community preparedness and response plans are essential in this context. Critical to these efforts is understanding the Estimated Times of Arrival (ETAs) of tsunamis, which dictate the vital window for post-earthquake actions and the likelihood of survival during an approaching tsunami. Our study aimed to assess the time available for communities in Aceh and nearby islands (Weh, Nasi, Breuh, Simeulue, Banyak) to respond and evacuate following an earthquake. We investigated ETA influenced by faults like Aceh-Andaman, Nias-Simeulue, and Batu segments, considering earthquake scenarios: 9.15 Mw (2004 tsunami reconstruction), 9.2 Mw, 8.9 Mw, and 8.6 Mw for Nias-Simeulue and Batu segments. Using the nonlinear shallow water equation (NSWE) model and numerical discretization with the finite difference method, we simulated tsunamis and projected arrival times. Our findings highlighted critical ETA ranges: 8–25 min on northern coasts, 19–37 min on western shores, 17–27 min on southwestern coasts, and 11–67 min on southern coasts. These results are essential for enhancing early warning systems and optimizing evacuation plans, and bolstering coastal community preparedness and resilience to tsunamis. Further studies are needed to conduct a comprehensive investigation of ETA, which includes potential rupture scenarios and a wider observation area, including expanding the modeling of tsunami generation mechanisms, which includes tsunamis generated by underwater landslides due to earthquakes or volcanic activity. Assessing ETA is pivotal for tsunami preparedness, contributing to more effective early warning systems and evacuation strategies. Integrating our ETA findings into policies will significantly enhance the preparedness and resilience of coastal communities in the face of ongoing tsunami risks. This study represents a valuable contribution to disaster risk reduction, offering actionable insights for safeguarding vulnerable coastal regions.

Keywords Coastal hydrodynamics · Tsunami model · Run-up · Evacuation time · Tsunami mitigation · Indian Ocean tsunami · Indonesia

Extended author information available on the last page of the article

1 Introduction

The oceanic seismic activity surrounding Sumatra (Indonesia) is characterized by a high degree of activity, leading to earthquakes that have the potential to cause tsunamis, as noted in several studies (Haridhi et al. 2018; Lange et al. 2018; Weller et al. 2012). The region has experienced numerous tectonic earthquakes that have caused tsunamis, as is extensively documented (Meltzner et al. 2006; Natawidjaja et al. 2006; Newcomb & McCann 1987). The impact of these disasters on the social and economic aspects of northern Sumatra, particularly Aceh, has been significant.

In the past two decades, the 2004 Indian Ocean tsunami has served as a benchmark for the world, with which to study the characteristics of tsunamis due to the massive destruction caused by the 2004 event. This was followed by a tsunami that hit the coast of Simeulue and Nias Islands on March 28, 2005, and the threat of a tsunami reoccurred in the region on April 11, 2012, when an earthquake with magnitudes of 8.6 and 8.2 Mw struck. The historical occurrences of tsunamis in Aceh have been proven by paleo-tsunami and archeological studies conducted by Monecke et al. (2008), Rubin et al. (2017), and Daly et al. (2019).

Regions that are at high risk of tsunamis require an efficient early warning system (EWS) to mitigate potential damage. In practice, evacuation responses from communities tend to be influenced by informal warning systems disseminated by government entities or other pertinent stakeholders. Natural indicators such as the receding tide at the beach often prompt individuals to evacuate (Muhari et al. 2012). For example, during the Palu-Donggala tsunami on September 28, 2018, several CCTV recordings circulated on social media documented the chronology of events at that time. The community immediately evacuated from buildings soon after the earthquake, but they did not immediately evacuate for the tsunami. People only responded to the evacuation when they saw other residents running away from the beach or when they directly witnessed the tsunami arriving on the mainland. This case highlights the gap regarding the community's response to early warning systems.

The provision of information on the arrival time of tsunamis is a crucial aspect for coastal communities to prepare adequately. This aspect is particularly crucial for near-field tsunamis, where flooding could occur swiftly, allowing for limited response time and planning of evacuation routes, destinations, and accommodations. To provide this information, ETA approaches are employed. ETA is essentially a computed prediction of the first wave of a tsunami's arrival after the earthquake that triggered it. Accurately predicting the ETA is crucial to ensure the safe and prompt evacuation of individuals at risk. The ETA ultimately determines the available evacuation time, which is a critical factor in determining the number of individuals that can be evacuated. Additionally, the correlation between the ETA and the number of evacuees has significant implications for various elements of evacuation planning, such as the identification of appropriate shelter locations, the design of evacuation routes, the dimensions of evacuation pathways, and the management of evacuation traffic flow.

This study delves deeper into the ETA of tsunamis caused by the Aceh-Andaman, Nias-Simeulue, and Batu segments. Its main objective is to chart out the critical response time that communities residing in the coastal areas of Aceh and strategic areas on outer islands of Sumatra, like Weh Island, Nasi Island, Breuh Island, Simeulue Island, and the Banyak Islands, have at their disposal to respond to, and to evacuate, after an earthquake. Fourteen ETA observation locations are discussed, categorized based on the regions of Aceh: Northern coast, Western coast, Southwestern coast, and

Southern coast. Additionally, the study also maps out the run-up and inundation distances for various simulated scenarios. While the relationship between the ETA and early warning system development is not explicitly discussed, the findings offer valuable insights into community preparedness. By linking the ETA findings with past evacuation experiences and assessments, significant factors for decision-making about self-evacuation can be identified. Thus, these findings hold significant practical implications for strengthening community resilience, even if they do not directly inform early warning systems.

2 Literature review

2.1 Tsunami risk

The Sumatra tectonic configuration plays a direct role in the seismic activity that triggered past tsunamis. The fault zoning in the oceanic area surrounding Sumatra commences from the Aceh-Andaman segment, which ruptured on December 26, 2004. Lay et al. (2005) predicted that the rupture along this segment was 1300 km long during the massive earthquake.

According to PusGen (2017), geodetic data show a slip rate of 4 mm/year, and the maximum magnitude can reach 9.2 Mw based on estimates. The fault line segmentation in Indonesia, as outlined in PusGen (2017), is shown in Fig. 1, which also depicts the epicenters of earthquakes that have caused tsunamis in Indonesia in the last two decades.

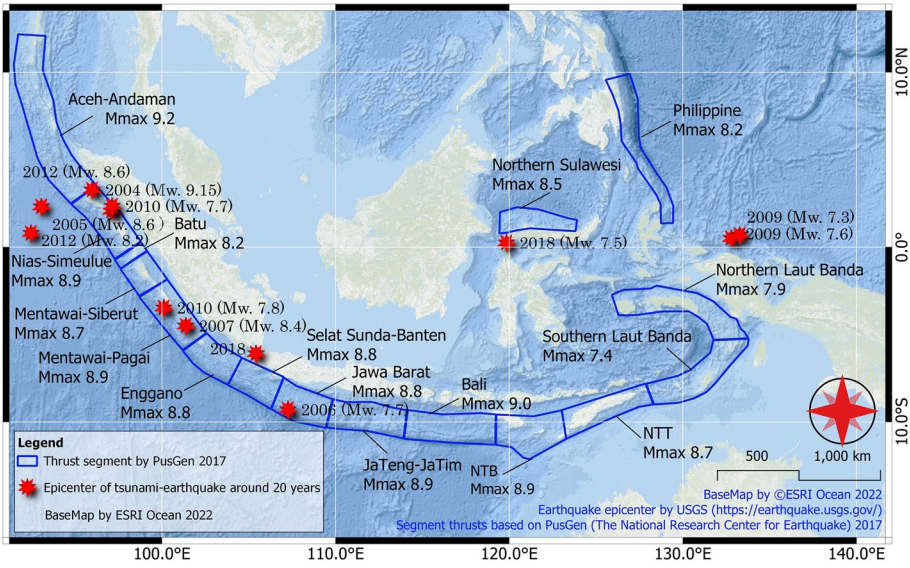

Fig. 1 Segmentation and maximum magnitude of subduction and tsunami earthquakes in Indonesia over the past two decades

2.2 The role of early warning systems

According to Basher et al. (2006) and UN/ISDR (2006), the effectiveness of an EWS relies on four fundamental elements: (1) understanding the potential risks; (2) technical monitoring and warning services; (3) effective dissemination and communication of warning knowledge to those individuals who may be at risk; and (4) public awareness and preparedness to respond to warnings. In addition to these four elements, for greater effectiveness, EWS must also consider cross-sectoral issues, including effective governance and institutions, multi-hazard approaches, local community involvement, gender perspectives, and cultural diversity (UN/ISDR 2006).

Oktari et al. (2014) assessed the effectiveness of the early warning system implemented in Aceh following the 2004 Indian Ocean tsunami. Their results demonstrated incremental advancements in the tsunami warning system but also revealed a lack of systematic policy and institutional commitment. The warning system, which comprised sirens, underwent testing during the April 11, 2012 earthquake. Regrettably, technical malfunctions and public misperceptions during the evacuation triggered panic amidst the evacuation process (Tim Kaji Cepat 2011). Additionally, a deficiency in grasping institutional roles and responsibilities, as well as a lack of coordination among response agencies, were recognized as inadequacies in developing the tsunami warning system in Aceh (Sufri et al. 2020).

2.3 The importance of estimated time of arrival (ETA)

Numerous studies have highlighted the factors that contribute to the level of fatalities in tsunami events. These factors are crucial in the development of evacuation research (Mas et al. 2012; Péroche et al. 2014; Wang et al. 2016) and encompass the following: the characteristics of the tsunami (arrival time and depth of flooding); the characteristics of the area affected (slope and elevation); mitigation efforts (evacuation zones and routes, disaster risk management); as well as personal characteristics (awareness of tsunami, knowledge of evacuation zones and routes, physical and mental abilities).

Several studies have aimed to model the ETA for various locations that are prone to tsunamis. The primary objective of those studies is to enhance the success rate of self-rescue efforts by accurately modeling ETA from past tsunami scenarios. Along with this, ETA information is also vital for investigating tsunami source mechanisms. Inverse theory, introduced by Satake and Kanamori (1991), is an example of studying earthquake sources based on tsunami waveform recorded by tide gauge stations. The need for arrival time variables from eyewitnesses in the field has also been emphasized by Shuto and Matsutomi (1995).

In addition, Titov et al. (2008) implemented a seismic event database to predict tsunami parameters, while Greenslade et al. (2011) applied a model to forecast tsunamis from a seismic scenario database. Jiménez (2010) presented an algorithm to quickly calculate the arrival time of the first tsunami, based on the linear path followed by the tsunami according to actual bathymetry, and this study was expanded by Jiménez et al. (2018). Those authors calculated the arrival time of the first tsunami and maximum tsunami height at actual tide gauge measurement points, both in the field and virtually. Syamsidik et al. (2015) conducted several modeling scenarios to determine ETA for various cities located on the west coast of Aceh. The tsunami initiation scenarios were determined based on several

past tsunami events starting from the 2004, 2005, 2007, 2010, and 2012 Sumatran coast tsunamis.

The outcomes derived from ETA modeling can serve as a robust framework for making policies to strengthen community preparedness, especially for individuals in regions susceptible to tsunamis. ETA data can give these communities invaluable insights, promoting quick and well-informed responses when tsunami early warnings are issued. This equips individuals with the knowledge needed to make timely decisions that can save lives and mitigate damage in the event of a tsunami (Chen et al. 2022). As a result, current policies must be adapted to include public awareness initiatives, specifically focused on educating the populace about effective responses based on the critical ETA information.

ETA modeling could also determine areas that demand immediate evacuation, making it an indispensable tool for shaping policies about establishing and maintaining evacuation infrastructure. Identifying these high-priority evacuation zones could ensure that resources are allocated where needed most, thereby enhancing the efficiency and effectiveness of evacuation procedures (Ito et al. 2021). Additionally, ETA mapping could discern regions that require early warnings more urgently than others. For instance, coastal areas near the tsunami's source may necessitate faster alerts than far-away coastal areas. This stratification enables the early warning system to dispatch alerts with appropriate levels of urgency, ensuring that communities at the most significant risk receive timely notifications that align with the imminent threat (Carvajal et al. 2018). This nuanced approach to alert dissemination could be instrumental in reducing the potential impact of tsunamis, and subsequently, guiding the development of policies that cater to the specific needs of different geographical zones.

3 Material and method

The occurrence of the colossal tsunami that struck Aceh in 2004 was triggered by a tectonic earthquake measuring 9.15 Mw (Chlieh et al. 2007; Meltzner et al. 2006). The epicenter was situated at 3.3° N, 95.8° E and had an epicenter depth of about 30 km. The earthquake caused a fault slip that was estimated at 12–15 m (Lay et al. 2005; Synolakis et al. 2005). The rupture segment of the 2004 tsunami was in the Aceh-Andaman zone. Consequently, the December 26, 2004 event was examined as a single scenario to reflect on the ETA on land at that time. The study concentrated on the coastal areas and outer islands of Aceh, which were chosen as the ETA assessment location due to the impact of previous tsunamis that affected these areas, including the Indian Ocean tsunami on December 26, 2004, the Nias-Simeulue tsunami on March 28, 2005, the Aceh tsunami on April 11, 2012 (small tsunami), and several other tsunamis that hit Aceh in the past (1907, 1861, 1797).

The simulation of tsunami initiation at source locations was conducted using the Mansinha and Smylie (1971) and Okada (1985) models in four modeling scenarios. These scenarios included the reconstruction of the 2004 Indian Ocean tsunami based on Koshimura et al. (2009) with a magnitude of 9.15 Mw, as well as three hypothetical scenarios based on updated fault segmentation with maximum magnitudes by PusGen (2017). The 9.15 Mw scenario was outlined to be representative of a historical event that had a profound impact on Aceh, specifically in 2004. Furthermore, three scenarios were designed to simulate potential tsunamis with different ruptures around Aceh's coasts, based on the assessment provided by PusGen (2017), as depicted in Fig. 1. The largest potential scenario was a 9.2-Mw earthquake scale occurring in the Aceh-Andaman segment,

with modifications in the large rupture dimension and adjusted fault angle, as referred to in Koshimura et al. (2009). Moreover, two scenarios in the Aceh-Andaman segment were simulated using multi-faults due to their segment lengths exceeding 1000 km. The Nias-Simeulue and Batu segments were simulated with a rupture scale of 8.9 Mw and 8.2 Mw, respectively. The moment magnitude scale in these modeling scenarios was calculated using the formula approach in the works of Hanks and Kanamori (1979) and Wells and Coppersmith (1994). A summary of earthquake parameters and complete scenarios are presented in Table 1.

In this investigation, we conducted an ETA mapping of the north-to-south Aceh coast in order to examine the characteristics of run-up. The study area is depicted in Fig. 2 and outlined in Table 2. We collected ETA observations on the primary island of Sumatra, which included Banda Aceh, Lhoknga, Weh Island in Sabang City, Nasi Island in Lamteng, and Breuh Island in Meulingge for the northern region. In a similar fashion, we performed ETA mapping on the western part of the south coast in Calang, Meulaboh, Nagan Raya, Susoh, Labuhan Haji, Tapaktuan, and Singkil. Moreover, we also observed the run-up characteristics in Simeulue Island, especially in Sinabang, as well as in the Banyak Islands, specifically on Tuangku Island. These 14 observation locations were specifically chosen to represent major urban areas densely populated along the north-to-south coastline of Aceh.

The investigation employed the Cornell Multi-grid Coupled Tsunami (COMCOT) model, which was initially created by Liu et al. (1998) to replicate the complete sequence of the tsunami, encompassing its generation, propagation, and run-up on the coastline. The model employs the finite difference method with an explicit staggered leap-frog scheme to solve the shallow water equation (SWE). The governing equations of the model are differentiated for both linear and nonlinear SWE. Specifically, the nonlinear SWE for Cartesian coordinates is articulated in accordance with the work of Wang (2009).

$$\frac{\partial \eta}{\partial t} + \left[\frac{\partial P}{\partial x} + \frac{\partial Q}{\partial y}\right] = -\frac{\partial h}{\partial t} \tag{1}$$

$$\frac{\partial P}{\partial t} + \frac{\partial}{\partial x}\left(\frac{P^2}{H}\right) + \frac{\partial}{\partial y}\left(\frac{PQ}{H}\right) + gH\frac{\partial \eta}{\partial x} + \frac{gn^2}{H^{\frac{7}{3}}}P\left(P^2+Q^2\right)^{\frac{1}{2}} = 0 \tag{2}$$

$$\frac{\partial Q}{\partial t} + \frac{\partial}{\partial x}\left(\frac{PQ}{H}\right) + \frac{\partial}{\partial y}\left(\frac{Q^2}{H}\right) + gH\frac{\partial \eta}{\partial y} + \frac{gn^2}{H^{\frac{7}{3}}}Q\left(P^2+Q^2\right)^{\frac{1}{2}} = 0 \tag{3}$$

The present study utilized the widely used SWE model, known for its accuracy in simulating long wave phenomena, particularly tsunamis. The COMCOT model was employed to simulate the initiation, propagation, and run-up of the tsunami on the coast. The SWE model was solved using the finite difference method with an explicit staggered leap-frog scheme. The SWE model utilizes various parameters such as water surface elevation, volume flux in the x and y directions denoted by (P, Q), respectively, and the total water depth represented by h, where the last term represents the roughness evaluated by the Manning coefficient (n). The model uses a uniform Manning roughness coefficient of 0.025.

The utilization of the SWE model in tsunami simulation has been extensively established through previous research endeavors. For instance, Muhari et al. (2012) employed this long wave model, which is based on the work of Imamura (1996), that analyzed the arrival time of the 2011 East Japan tsunami. Similarly, Syamsidik et al. (2015) adopted the COMCOT model to simulate numerous earthquake tsunami scenarios and to project

Table 1 Scenario for the initiation of tsunami source generation

No.	Thrust rapture/ type	Mw	L (km)	W (km)	Epicenter (◦)		D (km)	Dis (m)	Strike (◦)	Dip (◦)	Remark
					long	lat					
1	Aceh-Andaman segment/ multi-fault	9.15	200	150	94.400	3.030	10.0	14.0	323	15	The 2004 Indian Ocean tsunami reconstruction by Koshimura et al. (2009)
			125	150	93.320	4.480		12.6	335	15	
			180	150	92.870	5.510		15.1	340	15	
			145	150	92.340	7.140		7.0	340	15	
			125	150	91.880	8.470		7.0	345	15	
			380	150	91.900	11.000		7.0	7	15	
			1155	Total L (km)							
2	Aceh-Andaman segment/multi-fault	9.2	200	200	94.400	3.030	10.0	14.0	323	15	Hypothetical model
			135	200	93.320	4.480		12.6	335	15	
			205	200	92.870	5.510		15.1	340	15	
			160	200	92.340	7.140		7.0	340	15	
			170	200	91.880	8.470		12.6	345	15	
			430	200	91.900	11.000		15.1	7	15	
			1300	Total L (km)							
3	Nias-Simeulue segment/ single-fault	8.9	400	200	95.886	1.388	10.0	8.97	317	15	Hypothetical model
4	Batu segment/ single-fault	8.2	70	100	97.714	-0.485	10.0	9.14	319	15	Hypothetical model

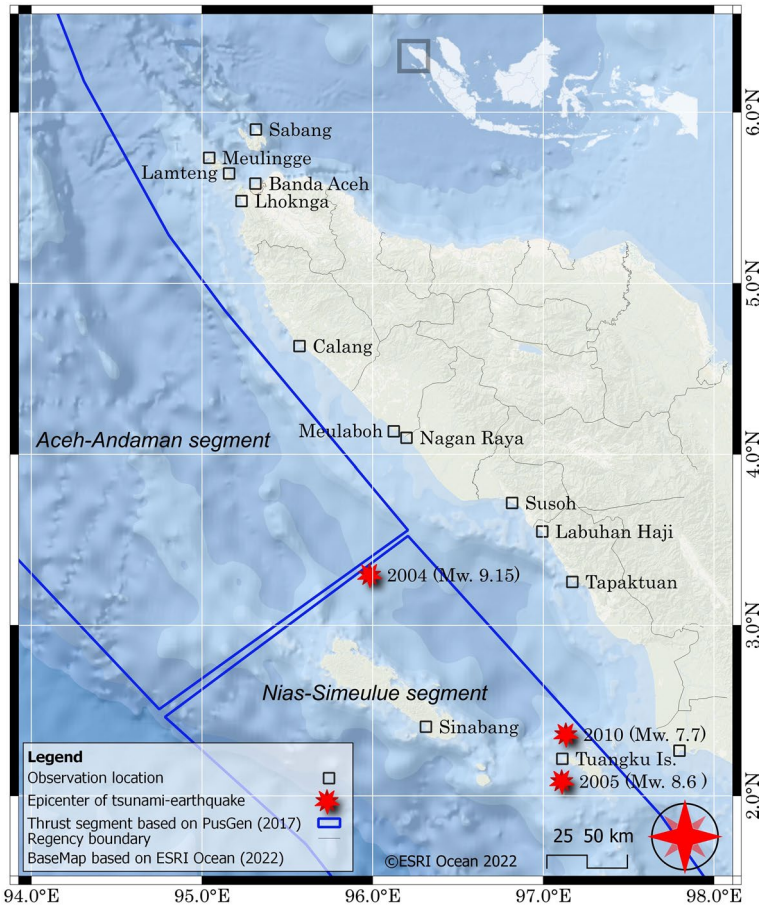

Fig. 2 Study location

the arrival time of the tsunami on the Aceh coast. Furthermore, Park and Cox (2016) conducted a study on the probabilistic evaluation of near-field tsunami hazards, which encompassed the arrival time of the tsunami in Seaside, Oregon (USA), using the ComMIT/MOST model from the work of Titov et al. (2011).

The computational domain was partitioned into four layers to achieve detailed computations, with the first layer encompassing the entire area from the source location to the coastline, and smaller insertion grids utilized to enhance resolution. Layer 4 was also subdivided into four regions, including the northern, western, southwestern, and southern parts of Aceh (as illustrated in Fig. 3). This approach facilitated a nuanced analysis of research findings, which are meticulously presented in Table 3, and led to more precise modeling of run-up and inundation on the coast. The data of the first domain were sourced from https://topex.ucsd.edu/cgi-bin/get_srtm30.cgi, and the data of the second domain were interpolated from the data of the first domain. For the third and fourth domains, data from https://tanahair.indonesia.go.id/demnas/#/batnas were

Table 2 Locations of ETA observation points

No	Obs. points	Long. (°)	Lat. (°)	Location	Region
1	OP-01	95.3132	5.5834	Banda Aceh (Lampulo Village)	Northern Aceh coast
2	OP-02	95.2319	5.4816	Lhoknga	
3	OP-03	95.3160	5.8996	Sabang City (Weh Island)	
4	OP-04	95.1590	5.6427	Lamteng (Nasi Island)	
5	OP-05	95.0425	5.7342	Meulingge (Breuh Island)	
6	OP-06	95.5715	4.6335	Calang	Western Aceh coast
7	OP-07	96.1240	4.1348	Meulaboh	
8	OP-08	96.1986	4.0969	Nagan Raya (PLTU)	
9	OP-09	96.8174	3.7170	Susoh (Blang Pidie)	Southwestern Aceh coast
10	OP-10	96.9943	3.5498	Labuhan Haji	
11	OP-11	97.1704	3.2544	Tapaktuan	
12	OP-12	97.7980	2.2649	Singkil	Southern Aceh coast
13	OP-13	96.3122	2.4053	Sinabang (Simeulue Island)	
14	OP-14	97.1116	2.2174	Tuangku Island (Banyak Islands)	

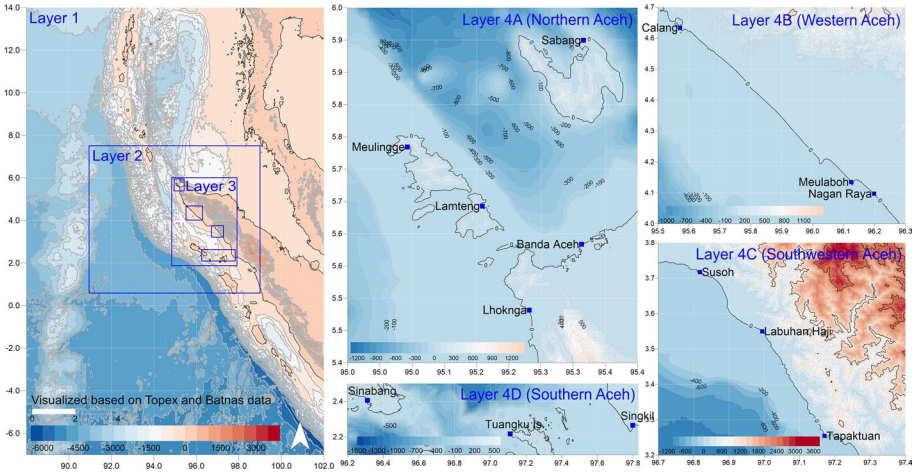

Fig. 3 Computational domain by applied nested grid configuration

utilized. Higher-resolution simulations of tsunami run-up and inundation in coastal areas were produced using nonlinear SWE calculations.

ETA observations were conducted at 14 distinct sites and yielded 56 data readings across four tsunami generation scenarios. The average depth recorded was below − 1 m. The methodology deployed to ascertain ETA was adapted from the work of Hayashi et al. (2011) which entailed categorizing arrival time into four wave phases, namely, the tsunami arrival phase, initial trough, local crest, and primary crest, as depicted in Fig. 4. The four wave phases represent the initial structure of a tsunami as it approaches the shore. During the Indian Ocean tsunami event, the wave arrival in Aceh's waters

Table 3 Division of computational domain and nested grid configuration

Computation domain	Layer 1	Layer 2	Layer 3	Layer 4A Northern Aceh	Layer 4B Western Aceh	Layer 4C South-western Aceh	Layer 4D Southern Aceh
Latitude (◦)	−7.00–14.00	1.80–7.60	1.90–6.00	5.40–5.95	4.00–4.70	3.20–3.80	2.10–2.50
Longitude (◦)	88.00–102.00	91.00–99.00	94.70–97.85	94.95–95.40	95.50–96.30	96.70–97.40	96.20–97.83
Grid number	841 × 1261	1441 × 1045	1702 × 2215	730 × 892	1297 × 1135	1135 × 973	2641 × 649
Grid size (m)	1110	370	123.33	41.11	41.11	41.11	41.11
Grid ratio	1	3	3	3	3	3	3
Time step (s)	1	1	0.5	0.25	0.25	0.25	0.25
SWE type	Linear	Linear	Nonlinear	Nonlinear	Nonlinear	Nonlinear	nonlinear
Data source	Topex	Topex	Batnas	Batnas	Batnas	Batnas	Batnas

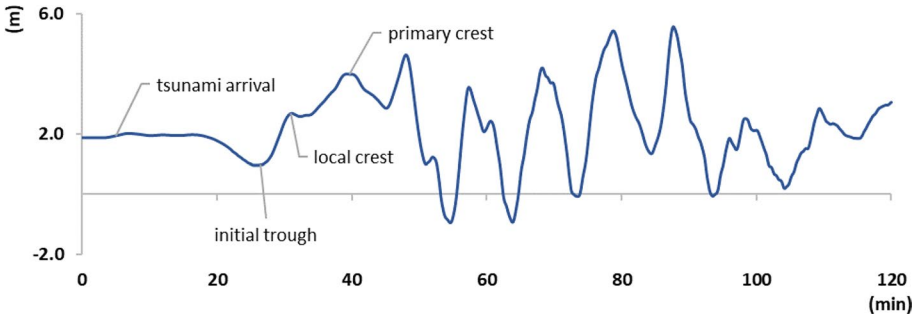

Fig. 4 Description of the time phases of tsunami arrival according to Hayashi et al. (2011)

commenced with the initial trough. However, not all tsunamis consistently initiate with this negative wave phase, because initiation depends on the rupture process. For instance, the 2010 Mentawai tsunami began with positive wave phases, such as the tsunami arrival and local crest, without the presence of an initial trough.

4 Results and discussion

4.1 Assessment of tsunami arrival time

The genesis of tsunamis as a source of production is predicated on the models developed by Mansinha & Smylie (1971) and Okada (1985). The computation of water surface deformation is subsequently evaluated in COMCOT using Eqs. (1) to (3). The Aceh-Andaman fault segment scenario is considered as the past event with a magnitude of 9.15 Mw, which yielded satisfactory results in tsunami modeling. The model verification was confirmed in Koshimura et al. (2009). The accuracy of the outcomes is affected by using multi-fault segmentation, rather than a single-fault approach, particularly for large-scale earthquakes (> 8 Mw). Based on the earthquake parameters listed in Table 3, Fig. 5 presents the tsunami initiation for four scenarios. At the time of the fault dislocation, the 9.15 Mw and 9.2 Mw scenarios generated negative waves of − 3.53 m and − 4.15 m, respectively, and positive waves of 10.78 m and 11.55 m, respectively. The Sumatra side also exhibited a prior decline in sea level for both scenarios, like the 2004 event. Borrero et al. (2006) reported that roughly 1.5 h after the earthquake, observers were astounded as they watched the ocean dramatically receding by over 500 m from its usual shoreline in Idi, around the east coast of Aceh. The waves split, with some heading east as a near-field tsunami for outer islands and Sumatra itself. The waves heading west were a far-field tsunami for Sri Lanka and the west coast of Africa. In contrast, the Nias-Simeulue fault created positive waves for outer islands such as Simeulue, Banyak Islands, and Nias Island. This condition was similar to the March 28, 2005 event (8.6 Mw), where the tsunami reached the coast after the earthquake stopped and immediately receded afterward in Lagundri Bay, Nias (Borrero et al. 2011). The 8.9 Mw scenario produced a maximum positive wave initiation of 2.92 m and a maximum negative wave initiation of − 2.05 m. On the other hand, for the Batu segment scenario with a magnitude of 8.2 Mw, a smaller tsunami formation occurred, with maximum

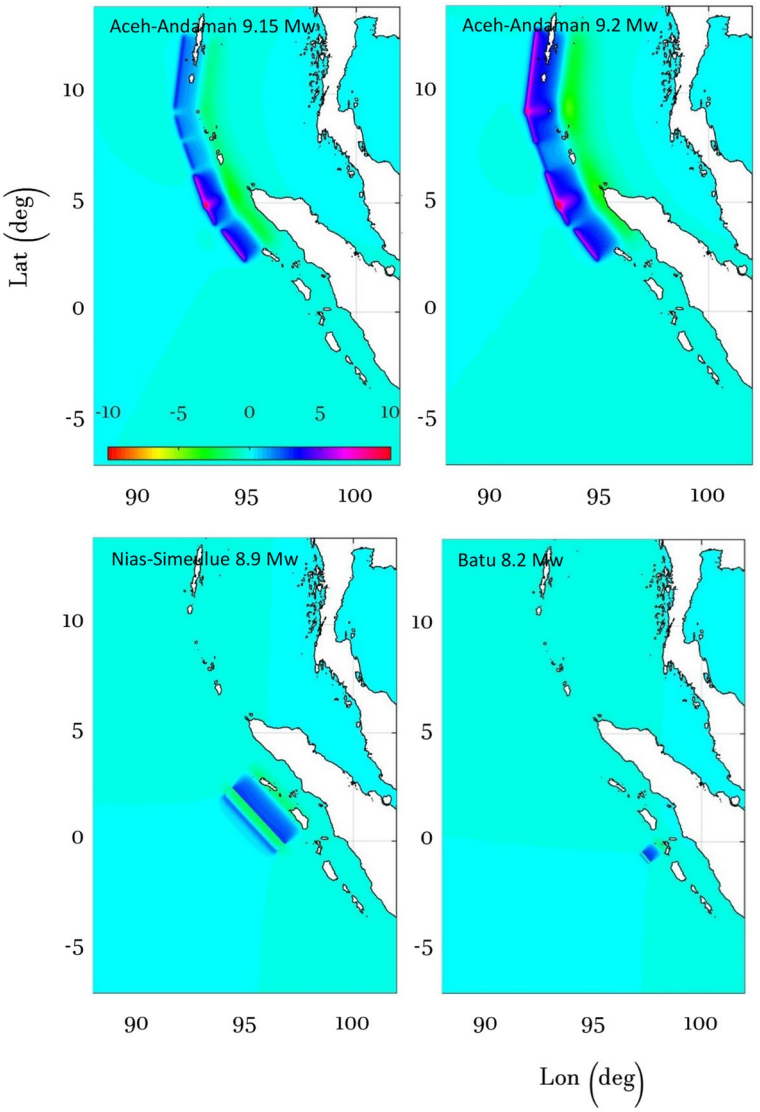

Fig. 5 Tsunami source characteristics for the four scenarios

positive and negative waves of 3.06 m and − 1.86 m, respectively. The ETA outcomes for the 14 examined locations are discussed based on regional division.

4.1.1 Characteristics of tsunami arrival time and inundation at the Northern Aceh coast

In this study, we investigated the characteristics of ETA in the densely populated northern zone of Aceh. The investigation was carried out at five different locations, namely, Banda Aceh, Lhoknga, Sabang, Lamteng, and Meulingge. The zone under investigation is situated

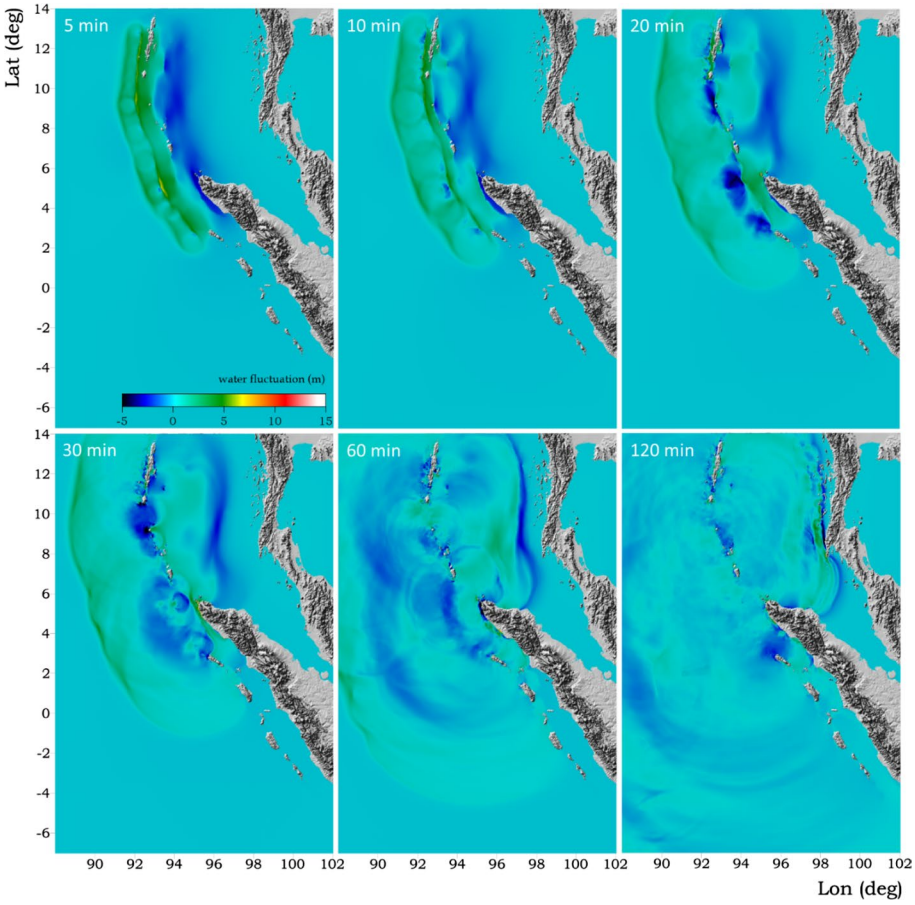

Fig. 6 Snapshot of the 9.2 Mw scenario showing tsunami wave transmission

near the Aceh-Andaman segment, which was subjected to the most severe impact during the 2004 Indian Ocean tsunami. Our analysis revealed that among the various scenarios which were considered, the rupture scenario of the Aceh-Andaman segment with a magnitude of 9.2 Mw resulted in the shortest arrival time and the largest run-up. The ETA of this scenario was marginally faster than the ETA of the 2004 Indian Ocean tsunami scenario and showed dissimilar outcomes for run-up and inundation on land. A visual representation of wave propagation from the source area to the run-up on land for the most severe impact scenario in this northern zone is presented in Fig. 6.

In Fig. 7, we present the outcomes of our observations and ETA, and maximum run-up range compilation for the four earthquake situations in this region. The variation observed in the tsunami's arrival time at different places underscores the intricate nature of tsunami propagation and the impact of various factors. The distance between the impacted area and the earthquake epicenter, which functions as the tsunami generation source, is one of the critical factors affecting the arrival time. This discovery is consistent with prior research that has highlighted the significance of distance in tsunami arrival (Catalán et al. 2015). Our modeling analysis outcomes for the most massive earthquake scenario in the

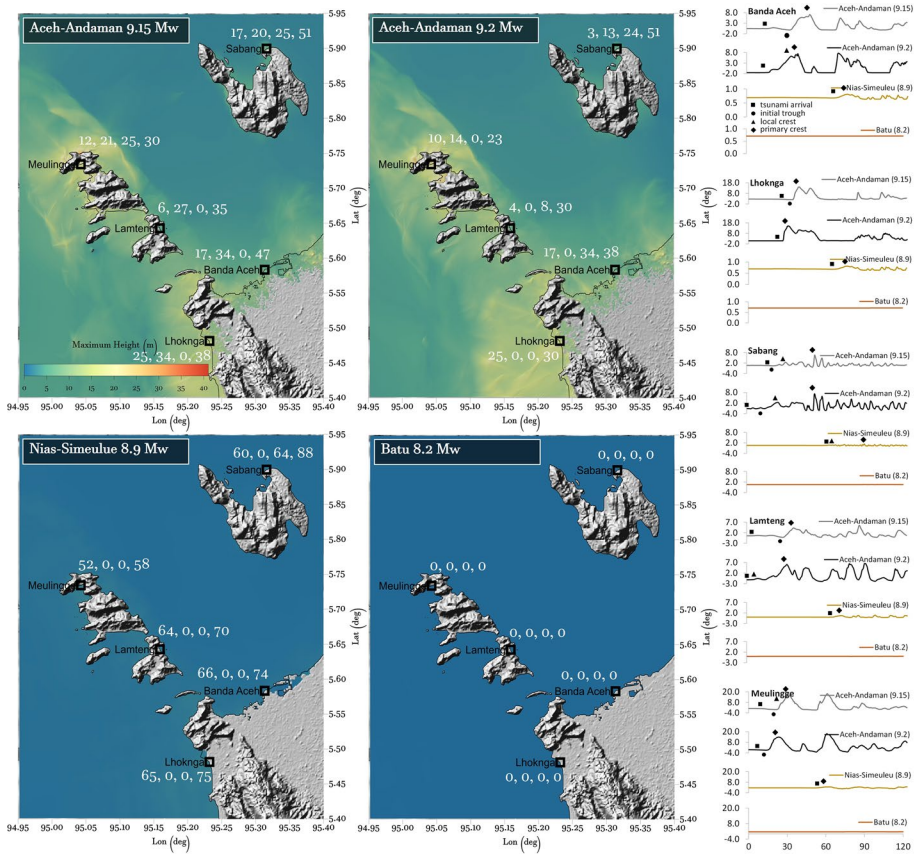

Fig. 7 Characteristics of tsunami arrival phases for Northern Aceh coast (tsunami arrival, initial trough, local crest, primary crest: minute)

Aceh-Andaman segment provide valuable insights into the specific arrival times at various locations. Sabang and Lamteng, which are situated closer to the subduction zone, experience an earlier arrival of the tsunami, with an average ETA of 3–4 min. This observation indicates that proximity to the source region can significantly influence the speed of tsunami propagation. On the other hand, Banda Aceh and Lhoknga, located farther away, experience delayed arrivals of 17 and 25 min, respectively. In the case of Indian Ocean tsunami, eyewitness accounts and stopped clocks indicated that the tsunami reached the Lhoknga coast approximately in the range of 13 to 21 min (Lavigne et al. 2009). The estimated arrival time for the outer islands of Sumatra is approximately 10 min. This delay can be attributed to their geographical location and the impact of local bathymetry, which can amplify or attenuate the tsunami waves as they propagate toward the coast. Previous studies have reported similar findings that highlight the role of local bathymetry in shaping the characteristics of tsunamis (Satake 1988; Murotani et al. 2015).

When comparing the reconstruction scenarios of the 2004 tsunami to the scenario of the largest earthquake, it is observed that there is no significant difference in the arrival time for a magnitude 9.2 earthquake. However, for the outer islands of Sumatra, the largest scenario demonstrates a slightly shorter time difference. This suggests that the

magnitude of the earthquake alone may not be the sole determinant of the arrival time. Instead, other factors such as local bathymetry and coastal topography should be considered for a comprehensive assessment. The third scenario, which involves the Nias-Simeulue fault segment, shows arrival times ranging from 60 to 66 min, with the fastest arrival observed at Meulingge after approximately 52 min following the earthquake. Discrepancies in arrival times within the same fault segment could be due to variations in fault geometry, rupture characteristics, and the influence of local bathymetry along the coastline. It is noteworthy that in our study, the Batu segment does not generate a tsunami for the northern coastal area of Aceh. This finding is consistent with previous research indicating that not all fault segments may produce significant tsunamis, and the specific characteristics of each segment need to be considered when assessing the tsunami hazard. Furthermore, wave properties, including wave height and wavelength, in segmented seafloor deformations are influenced not only by the overall width of the source but also by the number of segments and their relative sizes. A higher number of segments would result in shorter wave lengths and reduced wave heights on the surface, as per the results in the study by Shen et al. (2022).

Upon the initial arrival of a tsunami, the local peak wave phase is not immediately observed but rather followed by a negative wave or the early development of a trough phase. This phenomenon has been confirmed by Tursina et al. (2021) in their study in the same location, yielding similar results. In the case of the 2004 tsunami in Banda Aceh and Lhoknga, the fault mechanism within the subduction zone led to a receding sea level, with the sea retreating by up to 1 km, as demonstrated by Lavigne et al. (2013). Notably, although the subduction area and its rupture process play a significant role in generating local tsunamis in the western waters of Sumatra, not all large-scale near-field tsunamis are characterized by a receding sea level, as exemplified by the 2011 Japan tsunami (Muhari et al. 2012). Ren et al. (2019) have shown through their study on the effects of the rupture process tsunami source along the Manila Trench, which shares a similar rupture length with the 2004 Sumatra earthquake, that the kinematic source rupture process can lead to significant differences in wave patterns, amplitudes, and arrival times, influencing the amplitude and causing considerable delays in tsunami arrival times. Therefore, it is important to consider the specific conditions of each event when assessing the arrival and behavior of tsunamis.

The outcomes of the simulation also demonstrate that the existence of Nasi Island and Breuh Island in the northwest of Banda Aceh did not cause a significant delay in the arrival of the tsunami. The tsunami was recorded to commence at the 17th minute, and the primary waves arrived at their apex phase about 34–38 min after the earthquake. This occurrence can be attributed to the extensive rupture segment, which spans approximately 1300 km, and even reaches the Nicobar and Andaman Islands. The length and features of this fault rupture segment play a critical role in determining the propagation of tsunamis and their arrival time. According to witnesses, in the 2004 event, it took approximately 25 min for the tsunami water to reach the area near the Grand Mosque after the earthquake (Borrero et al. 2006). This suggests that the initial impact of the tsunami was relatively rapid, as the water traveled from the ocean to the center of Banda Aceh in around 25 min.

The outcomes of the run-up simulation display considerable variations depending on the site of the investigation and the seismic scenarios under consideration. In Banda Aceh, the tsunami height resulting from a seismic incident like the 2004 catastrophe varies between 10 and 12 m. Prior investigative reports on the 2004 event revealed an estimated tsunami height of 12 m along the coast of Banda Aceh, including Ulee Lheue (Borrero et al. 2006; Tsuji et al. 2006). Regarding the extent of flooding in Banda Aceh, houses located

approximately 2 km from the shoreline were swept away, while those situated beyond 3 km were less affected, and the flooding persisted for roughly 5 to 6 km inland (Tsuji et al. 2006). The first author, who personally witnessed the tsunami, observed the extent of the flooding during the evacuation and noted that the floodwaters reached 4 km along T. Hasan Dek Street, particularly before the Simpang Surabaya bridge, Banda Aceh.

In the Lhoknga region, the magnitude of the tsunami was notably greater, falling within the range of 20 to 30 m. The highest recorded tsunami run-up of 34.5 m was documented in this area by Tsuji et al. (2006) during their post-survey activities. The northern islands of Banda Aceh also experienced significant tsunami heights, with Breuh Island struck by a tsunami of 30 m and Nasi Island witnessing heights ranging from 10 to 12 m. According to Borrero et al. (2006), post-survey data further indicated that the tsunami height on Breuh Island reached between 13 and 20 m in the Lampuyang area, while Nasi Island recorded a height of 10 m. However, Sabang city was only affected by a tsunami with a height of 5 to 6 m, unlike Pulau Weh.

For the 9.2 Mw scenario, the recorded tsunami height on land was higher on average. Nonetheless, this value could have been even more significant if the modeling had utilized a finer data resolution. Conversely, the other two scenarios did not yield substantial tsunami heights for the northern region of Aceh.

4.1.2 Characteristics of tsunami arrival time and inundation at western Aceh coast

The ETA measurements were carried out in Calang, Meulaboh, and Nagan Raya, which are representative of the developing region on the west coast of Aceh, as illustrated in Fig. 8. The tsunami arrived in Calang earlier and was triggered by the tsunami arrival phase at 19

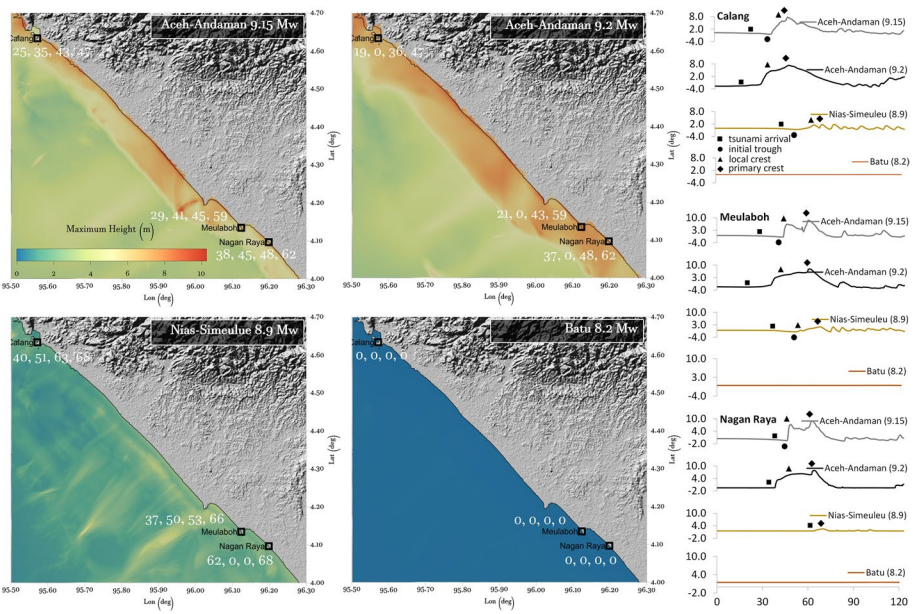

Fig. 8 Characteristics of tsunami arrival phases for Western Aceh coast (tsunami arrival, initial trough, local crest, primary crest: minute)

and 25 min for the Aceh-Andaman segment scenarios with magnitudes of 9.2 Mw and 9.15 Mw, respectively. The local crest phase followed at 36 and 43 min, and the primary crest at 47 min. In Meulaboh, waves were detected at 21 and 29 min for both Aceh-Andaman scenarios, with the initial wave phase starting with the tsunami arrival. The measurement point in Nagan Raya, located about 7 km south of Meulaboh, recorded the tsunami arrival at 37–38 min, followed by the local crest phase for this area. In the Nias-Simeulue segment rupture scenario, the tsunami reached Meulaboh 37 min earlier, Calang at 40 min, and Nagan Raya at 62 min. However, no tsunami was detected on the mainland of this west coast area for the Batu segment scenario.

The modeling results presented in Fig. 8 also provide valuable insights into the run-up patterns and tsunami heights for different earthquake scenarios along the coastal areas of Meulaboh, Nagan Raya, and Calang. The simulations reveal that the tsunami heights along the coastlines of Meulaboh and Nagan Raya reached remarkable values of 10 m, while they attained 8 m in Calang for earthquake magnitudes of 9.15 and 9.2 Mw. However, the run-up height was relatively lower, around 2 m, for the earthquake magnitude of 8.9 Mw along the coastal zone, and no significant run-up was observed for the 8.2 Mw earthquake scenario. These results highlight the strong correlation between earthquake magnitude and tsunami heights, emphasizing the importance of considering various seismic scenarios in coastal risk assessments. Comparison of these findings with historical data indicates that the catastrophic 2004 Indian Ocean tsunami caused significant damage to Meulaboh and its environs, with recorded tsunami heights of 12–14 m in Calang, confirmed by broken tree branches in the hilly areas near the city (Tsuji et al. 2006).

4.1.3 Characteristics of Tsunami arrival time and inundation at Southwestern Aceh coast

The southwestern Aceh coastal region is represented by three measurement locations, namely, Susoh, Labuan Haji, and Tapaktuan. Tapaktuan experienced the tsunami earlier than the other two locations, at 7 min for the 9.2 Mw earthquake scenario. Similarly, for the 8.6 Mw and 9.15 Mw scenarios, the arrival time of the tsunami was recorded at the same location at 10 and 14 min, respectively. In the Aceh-Nias segment scenario, Susoh and Labuan Haji recorded the arrival time of the tsunami at 27 and 43 min, respectively. As such, it can be inferred that Tapaktuan has the shortest wave arrival time in the southwestern Aceh region for both the Aceh-Andaman and Nias-Simeulue segment ruptures. Furthermore, in the Batu segment rupture scenario, Tapaktuan witnessed the arrival of the tsunami after 72 min, with no signs of its arrival at the other two locations.

The results of the model reveal significant discrepancies in the maximum heights of tsunamis along the southwestern coast of Aceh, contingent upon the specific earthquake scenarios considered. The Aceh-Andaman fault segment scenario generated maximum tsunami heights ranging from 5 to 7 m on the coastal terrain. The relatively lower levels of inundation observed in this area can be attributed to the greater distance of the source of generation in comparison to the coastal regions located in the west and north. For instance, in Tapaktuan, the tsunami heights only exceeded about 1–2 m on the coastal land. In contrast, Fig. 9 clearly demonstrates that the Nias-Simeulue segment scenario resulted in even higher tsunami heights (ranging from 5 to 6 m) for this coastal area. Notably, the Batu fault segment scenario exhibited only minor fluctuations and small ripples in Tapaktuan.

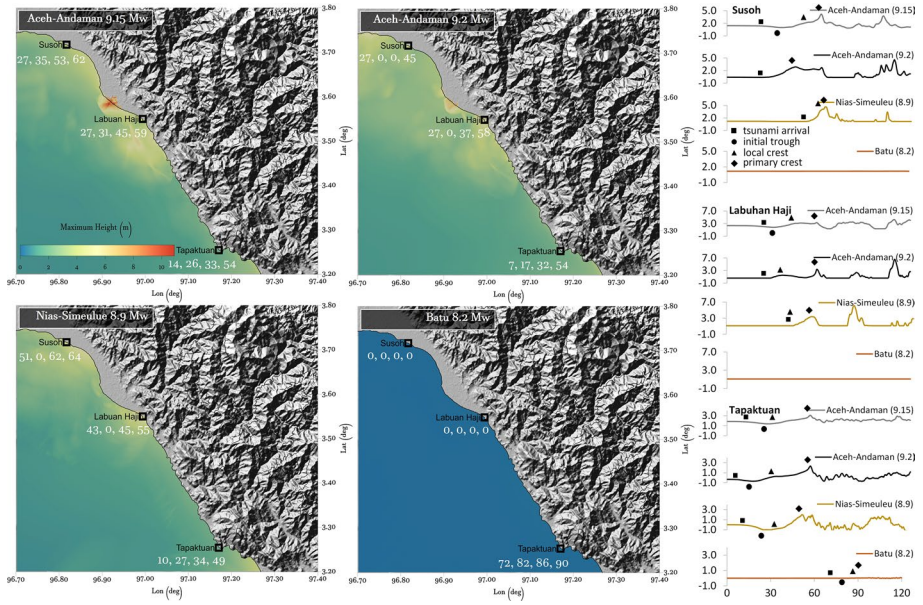

Fig. 9 Characteristics of tsunami arrival phases for the Southwestern Aceh coast (tsunami arrival, initial trough, local crest, primary crest: minute)

4.1.4 Characteristics of Tsunami arrival time and inundation at southern Aceh coast

Sinabang, Banyak Islands, and Singkil are designated as the locations for ETA assessment in the Southern Aceh coast region. In the instance of the Nias-Simeulue segment rupture scenario, the tsunami reached Sinabang on Simeulue Island before any other location, arriving 11 min after the onset of the rupture. The initial phase of the tsunami arrival was followed by the local crest and primary crest phases at 14 and 24 min, respectively. Additionally, the Banyak Islands and Singkil experienced an earlier arrival of the tsunami in comparison to the other three scenarios. In this zone, the Batu segment rupture scenario recorded the tsunami arrival at all three assessment locations, occurring at 58, 59, and 99 min for Sinabang, Banyak Islands, and Singkil, respectively.

The results obtained from the modeling outcomes of the southern coastal region of Aceh have indicated that the tsunami heights are relatively greater in comparison to the scenarios associated with the Nias-Simeulue fault segment. Through the simulations, it has been established that the tsunami heights can escalate up to 7 m in Sinabang, Simeulue Island, and up to 5 m in the Banyak Islands (refer to Fig. 10). On the other hand, the Aceh-Andaman fault segment resulted in lower run-up heights and inundation distances. For instance, in Singkil, the recorded tsunami height was approximately 0.6 m in the scenario involving the Batu fault segment. These findings emphasize the variation in tsunami impacts along the Aceh coast, and highlight the importance of incorporating specific fault segments in the modeling process.

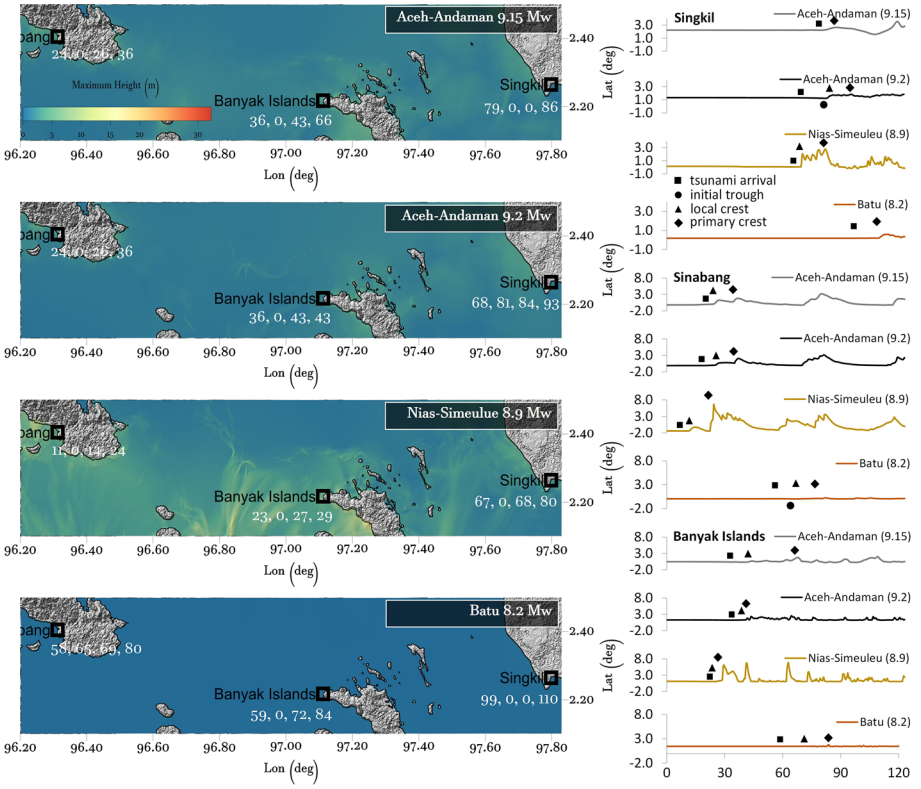

Fig. 10 Characteristics of tsunami arrival phases for Southern Aceh coast (tsunami arrival, initial trough, local crest, primary crest: minute)

4.2 Estimated time of arrival (ETA) evaluation for tsunami preparedness

Determination of the optimal estimated time of arrival (ETA) of a tsunami stands as a pivotal factor in formulating robust mitigation strategies, particularly hinged upon the nuances of wave phases and the varied mechanisms instigating tsunami generation. Examining the scenario within the Aceh-Andaman fault segment, the observation of an early arrival of the initial trough phase in Banda Aceh, with an ETA of 34 min, is noteworthy. However, it is crucial to note the observed oscillations in tsunami arrival phases, occurring as early as 17 min post-event. This variability in arrival times prompts consideration of alternative definitions of ETA, such as when the wave height reaches 0.5 m above mean sea level (MSL) near the coast (BMKG 2012). Notably, Syamsidik et al. (2015) employed this criterion, establishing a 35-min ETA for Banda Aceh, based on the 2004 tsunami reconstruction modeling scenario, and employing a reading point set at a depth of 10 m. Moreover, the Aceh Disaster Management Agency, Badan Penanggulangan Bencana Aceh (2019), outlined an ETA range of 10 to 20 min for an Aceh-based tsunami, specifically linked to potential scenarios associated with the 9.2 Mw Aceh-Andaman segment. This multifaceted understanding of ETA proves pivotal for disaster management teams, affording them the necessary insights to mount swift and effective responses, ultimately minimizing the potential for human casualties and mitigating property damage in the wake of a tsunami event.

Given the circumstances, the phase of tsunami arrival is of utmost importance, particularly for communities located on the coast during an earthquake. The timely identification and precise forecast of the arrival time of a tsunami are imperative to ensure effective evacuation and preparedness measures that can safeguard coastal populations from the catastrophic effects of tsunamis. Consequently, we have determined the critical time of arrival of the tsunami that poses a significant threat (termed as ETA_c) for the Aceh coast region. The critical ETA determination is based on observing the wave phase forms arriving at coastal land from four simulated rupture scenarios. We selected the earliest arrival time by comparing the wave phase characteristics, specifically focusing on positive wave phases, encompassing either tsunami arrival or immediate local crests. This determination also considers the initial trough phase, a component of ETA, during which the tsunami experiences an initial recession (negative wave) followed by the subsequent local crest. The critical time obtained has been systematically arranged in Table 4, considering the strategically placed measuring locations employed in the simulation.

Table 4 provides an overview of the ETA at several locations along the coast of Aceh. The analysis results show that the areas in the Northern Aceh coast, Lamteng, with the shortest ETA (8 min), show significant challenges in early warning and evacuation. On the Western Aceh coast, Calang has the shortest ETA (19 min). Calang is one of the areas on the west coast of Aceh Province that experienced the worst damage from the tsunami and earthquake disaster in 2004. Meanwhile, the Southwestern Aceh coast showed variations, with Tapaktuan having the shortest ETA (17 min). The Southern Aceh coast region, especially Sinabang, with an ETA of 11 min, indicates the need for a high level of vigilance. This analysis provides valuable insights for designing more effective tsunami mitigation strategies, considering highly variable arrival times of tsunami waves across the Aceh region. Factors such as distance from potential tsunami sources, topography, and geographic structure are key in designing optimal early warning systems and efficient evacuation planning.

The reception of tsunami information on the mainland in a timely manner is of great importance to reduce the loss of life and property. This study presented a method of reading ETA by installing tsunami sensors in shallow waters, like harbors, to monitor fluctuations in wave height. To receive information on tsunami occurrence more quickly, sensors could be installed in open seas or on outermost islands facing the mainland. Furthermore,

Table 4 Recapitulation of critical tsunami arrival times along Aceh coast

Location/ETA_c (min)	*Northern Aceh coast*				
	Banda Aceh	Lhoknga	Sabang	Lamteng	Meulingge
	17	25	13	8	10
	Western Aceh coast				
	Calang	Meulaboh	Nagan Raya		
	19	21	37		
	Southwestern Aceh coast				
	Susoh	Lab. Haji	Tapaktuan		
	27	27	17		
	Southern Aceh coast				
	Singkil	Sinabang	Banyak Is		
	67	11	23		

placing sensors on fishing vessels could enable the immediate transmission of information to land when fishermen are at sea during a tsunami (Nurendyastuti et al. 2022). A number of developments have been made in early tsunami detection, including high-frequency radar detection based on tsunami speed, as demonstrated during the 2011 Tohoku tsunami (Lipa et al. 2019). Additionally, real-time tsunami forecasting based on earthquake parameters has been developed, as illustrated for the 2012 Aceh tsunami by Wang et al. (2012).

The ETA evaluation is a critical component in reinforcing regional efforts to lessen the risks of natural hazard-caused disasters. In highly populated urban areas like Banda Aceh and Meulaboh, there exists a narrow window of approximately 17–21 min following an earthquake, known as the "golden time," when decisions regarding evacuation can be made. The effectiveness of such measures is highly dependent on the populace's understanding of disaster management or prior experiences. The success of self-rescue efforts is determined by factors such as the time available for evacuation, the distance to the designated evacuation zone, and the transportation methods used (Chen et al. 2022). Appropriate use of this crucial time necessitates psychological preparedness to gather information and make decisions regarding evacuation, as well as logistical preparations like packing essential items, such as valuables and documents, for transportation during evacuation (Kubisch et al. 2020). These actions should be consistent with the ETA applicable to each susceptible region facing the risk of tsunami arrival. The optimal utilization of the critical period entails an individual's psychological preparedness to acquire current status information, followed by the process of decision-making concerning evacuation, as posited by Lindell et al. (2018), National Research Council (2011), and Wood et al. (2018). This is augmented by logistical arrangements and packing, including the collection of vital documents to be carried during the evacuation process, as stated by Lindell et al. (2005). These actions necessitate modification in accordance with the ETA available for each region susceptible to tsunamis.

ETA evaluation would make a significant contribution to the development of better tsunami mitigation policies. The results of the ETA evaluation provide potent insights into how communities should respond effectively to the tsunami threat. Therefore, it is essential to ensure that existing policies integrate public awareness campaigns regarding effective responses based on ETA mapping results. By strengthening community understanding of ETA, the policy could improve the preparedness and protection of coastal communities.

ETA modeling also allows the identification of areas that require evacuation more quickly, which can be used to develop policies regarding the construction and maintenance of evacuation infrastructure. By knowing regions requiring special attention in evacuation, the government can allocate resources more efficiently and ensure that evacuation infrastructure is well maintained. This can contribute to community safety and reduce potential losses due to tsunamis.

ETA mapping results can also help determine areas that require early warning more quickly than others. For example, coastal regions near a tsunami source may require warnings more rapidly than areas further away. This more granular approach allows early warning systems to send alerts with appropriate priority levels so that communities most at risk are notified promptly regarding impending threats. This more nuanced approach can help mitigate the potential impacts of tsunamis, and as a result, guide the development of policies that address the specific needs of different geographic zones.

The present study offers valuable research regarding the determination of critical arrival times of tsunamis along the Aceh coast area. However, it is crucial to acknowledge several limitations. First, the accuracy of the model-based travel times could be affected by uncertainties in the earthquake source parameters and bathymetry data utilized in the

simulations. Second, the study focuses solely on potential fault ruptures triggered by earthquakes, neglecting other significant tsunami sources, such as landslides or marine volcano explosions. The simplifications in the simulation model, the limited spatial resolution, and the assumptions about wave propagation characteristics could impact the precision and generalizability of the findings. The availability and quality of data, in conjunction with the omission of external factors such as climate change, could also affect the robustness of the results. Furthermore, a potential avenue for further development in this research lies in conducting a more detailed investigation focused on inland areas concerning the tsunami inundation duration for evacuation purposes. Understanding the relationship between the characteristics of a tsunami's inland propagation and the various land use patterns is crucial in determining the flow velocity. Exploring the coastal community's psychological dimensions in decision-making processes regarding evacuation is also essential. This qualitative study would inherently vary depending on the coastal community's level of disaster awareness and knowledge. Hence, classifying communities based on their disaster experience, whether they have encountered disasters, are newcomers, or reside in areas with intense disaster education and outreach, could provide valuable insights for future research endeavors.

5 Conclusion

The momentous instance of the arrival of the tsunami on the northern shorelines was ascertained to be approximately between 8 to 25 min, while on the western shores, it was observed to be about 19 to 37 min; similarly, on the southwestern coasts, it was identified to be around 17 to 27 min, and on the southern coastlines, it was found to be within a range of 11 to 67 min. These estimates have been determined through the evaluation of the ETA characteristics during the tsunami arrival phase and the local trough, in the context of predefined scenarios. The evaluation of ETA in regions prone to tsunamis is a crucial aspect of initiatives aimed at reducing disaster risk, since it directly affects the availability of evacuation time. However, the effectiveness of evacuations also depends heavily on the ability of communities to adapt their behavior in accordance with the ETA allocations provided.

In the context of tsunami preparedness, ETA evaluation plays a crucial role. It offers valuable insights into how communities could respond more effectively to tsunami threats. Additionally, ETA modeling helps identify areas requiring swifter evacuation, and ETA mapping results assist in pinpointing regions needing early warnings. Integrating ETA evaluation findings into tsunami mitigation policies could enhance community preparedness, optimize resource allocation, and ensure timely early warnings, all with the ultimate goal of minimizing the adverse impacts of tsunamis and safeguarding coastal communities' lives and property.

Additional comprehensive investigations of ETA are necessary, encompassing potential rupture scenarios and wider observation regions. This can be complemented by the extension of the modeling of tsunami generation mechanisms, which incorporates tsunamis produced by submarine landslides resulting from earthquakes (like the 2018 Palu-Donggala tsunami) or volcanic activities (like the 2018 Anak Krakatau tsunami). The understanding of the complexities of tsunami generation and propagation is critical for enhancing disaster preparedness and reducing risks in exposed coastal areas. As research advances, the prioritization of enhancing community awareness and readiness for possible tsunami events is also imperative to increase the efficacy of evacuation tactics, and minimize the impacts of these natural hazard-caused disasters.

Acknowledgements We would like to express our deep appreciation to Prof. T. Faisal Fathani from Universitas Gadjah Mada for his invaluable contribution to this paper. His meticulous review of the writing style and organization significantly enhanced the quality and clarity of the content. We would also like to extend our heartfelt thanks to Ms. Tursina from State Polytechnic of Lhokseumawe for her invaluable advice and guidance during the numerical modeling phase of this research. Her insights and expertise greatly contributed to the success of this project.

Author contributions B contributed to conceptualization, simulation, data analysis, visualization, writing–original draft, and editing the manuscript. RSO helped in writing–original draft, and improving the quality of the manuscript.

Funding The authors declare that no funds, grants, or other support were received during the preparation of this manuscript.

Declarations

Conflict of interest The authors declare that they have no conflict of interest.

Ethical approval Not applicable.

Consent for publication All authors approved the publication of this study.

References

Badan Penanggulangan Bencana Aceh (2019) Rencana Kontinjensi Gempa Bumi dan Tsunami Provinsi Aceh 2019

Basher R, Page J, Woo J, Davies ML, Synolakis CE, Farnsworth AF, Steacey S (2006) Global early warning systems for natural hazards: Systematic and people-centred. Philosoph Trans Royal Soci a: Math, Phys Eng Sci, Royal Soci 364(1845):2167–2182. https://doi.org/10.1098/rsta.2006.1819

BMKG (Meteorological Climatological and Geophysical Agency). (2012). Tsunami Early Warning Service Guidebook for InaTEWS (Second Edition). Badan Meteorologi Klimatologi & Geofisika (BMKG). https://www.gitews.org/tsunami-kit/en/E3/tool/Tsunami%20Early%20Warning%20Service%20Guidebook%20for%20InaTEWS.pdf

Borrero JC, Synolakis CE, Fritz H (2006) Northern Sumatra field survey after the December 2004 great Sumatra earthquake and Indian Ocean tsunami. Earthq Spectra. https://doi.org/10.1193/12206793

Borrero JC, McAdoo B, Jaffe B, Dengler L, Gelfenbaum G, Higman B, Hidayat R, Moore A, Kongko W, Lukijanto PR, Prasetya G, Titov V, Yulianto E (2011) Field survey of the March 28, 2005 Nias-Simeulue earthquake and Tsunami. Pure Appl Geophys 168(6–7):1075–1088. https://doi.org/10.1007/s00024-010-0218-6

Carvajal M, Araya-Cornejo C, Sepúlveda I, Melnick D, Haase JS (2019) Nearly instantaneous tsunamis following the Mw 7.5 2018 Palu earthquake. Geophys Res Lett 46(10):5117–5126. https://doi.org/10.1029/2019GL082578

Catalán PA, Aránguiz R, González G, Tomita T, Cienfuegos R, González J, Shrivastava MN, Kumagai K, Mokrani C, Cortés P, Gubler A (2015) The 1 April 2014 Pisagua tsunami: observations and modeling. Geophys Res Lett 42(8):2918–2925. https://doi.org/10.1002/2015GL063333

Chen C, Wang H, Lindell MK, Jung MC, Siam MRK (2022) Tsunami preparedness and resilience: evacuation logistics and time estimations. Transp Res D Transp Environ 109:103324. https://doi.org/10.1016/J.TRD.2022.103324

Chlieh M, Avouac JP, Hjorleifsdottir V, Song TRA, Ji C, Sieh K, Sladen A, Hebert H, Prawirodirdjo L, Bock Y, Galetzka J (2007) Coseismic slip and afterslip of the great Mw 9.15 Sumatra-Andaman earthquake of 2004. Bull Seismol Soc Am. https://doi.org/10.1785/0120050631

Daly P, Sieh K, Seng TY, McKinnon EE, Parnell AC, Ardiansyah FRM, Ismail N, Nizamuddin MJ (2019) Archaeological evidence that a late 14th-century tsunami devastated the coast of northern Sumatra and redirected history. Proc Natl Acad Sci USA 116(24):11679–11686. https://doi.org/10.1073/pnas.1902241116

Greenslade DJM, Allen SCR, Simanjuntak MA (2011) An evaluation of tsunami forecasts from the T2 scenario database. Pure Appl Geophys 168(6–7):1137–1151. https://doi.org/10.1007/s00024-010-0229-3

Hanks TC, Kanamori H (1979) A moment magnitude scale. J Geophys Res Solid Earth 84(B5):2348–2350. https://doi.org/10.1029/JB084iB05p02348

Haridhi HA, Huang BS, Wen KL, Denzema D, Agung Prasetyo R, Lee CS (2018) A study of large earthquake sequences in the Sumatra subduction zone and its possible implications. Terr Atmospheric Ocean Sci 29(6):635–652. https://doi.org/10.3319/TAO.2018.08.22.01

Hayashi Y, Tsushima H, Hirata K, Kimura K, Maeda K (2011) Tsunami source area of the 2011 off the Pacific coast of Tohoku Earthquake determined from tsunami arrival times at offshore observation stations. Earth Planets Space 63(7):809–813. https://doi.org/10.5047/eps.2011.06.042

Imamura F (1996) Review of tsunami simulation with a finite difference method. In: Yeh H, Liu P, Synolakis C, Eds., Long-Wave Run-up Models, World Scientific 43–87. https://cir.nii.ac.jp/crid/1574231875748970112.bib?lang=en

Ito E, Kosaka T, Hatayama M, Urra L, Mas E, Koshimura S (2021) Method to extract difficult-to-evacuate areas by using tsunami evacuation simulation and numerical analysis. Int J Disaster Risk Reduct 64:102486. https://doi.org/10.1016/j.ijdrr.2021.102486

Jiménez C, Carbonel C, Rojas J (2018) Numerical procedure to forecast the tsunami parameters from a database of pre-simulated seismic unit sources. Pure App Geophys 175(4):1473–1483. https://doi.org/10.1007/s00024-017-1660-5

Jiménez C (2010) Software for Determination of Occurrence of Tsunamis. Bol. Soc. Geol. Perú 104:25–31. https://www.dhn.mil.pe/files/cnat/pdf/articulos/Software%20para%20ocurrencia%20de%20maremotos.pdf

Koshimura S, Oie T, Yanagisawa H, Imamura F (2009) Developing fragility functions for tsunami damage estimation using numerical model and post-tsunami data from banda aceh, Indonesia. Coas Eng J 51(3):243–273. https://doi.org/10.1142/S0578563409002004

Kubisch S, Guth J, Keller S, Bull MT, Keller L, Braun AC (2020) The contribution of tsunami evacuation analysis to evacuation planning in Chile: applying a multi-perspective research design. Int J Disaster Risk Reduct. https://doi.org/10.1016/j.ijdrr.2019.101462

Lange D, Tilmann F, Henstock T, Rietbrock A, Natawidjaja D, Kopp H (2018) Structure of the central Sumatran subduction zone revealed by local earthquake travel-time tomography using an amphibious network. Solid Earth 9(4):1035–1049. https://doi.org/10.5194/se-9-1035-2018

Lavigne F, Paris R, Grancher D, Wassmer P, Brunstein D, Vautier F, Leone F, Flohic F, de Coster B, Gunawan T, Gomez C, Setiawan A, Cahyadi Fachrizal R (2009) Reconstruction of tsunami inland propagation on December 26, 2004 in Banda Aceh, Indonesia, through field investigations. Pure Appl Geophys 166(1–2):259–281. https://doi.org/10.1007/s00024-008-0431-8

Lavigne F, Paris R, Leone F, Gaillard JC, Morin J (2013) Indian Ocean Tsunami, 2004. In: Bobrowsky PT (ed) Encyclopedia of natural hazards. Springer, Netherlands, pp 529–535. https://doi.org/10.1007/978-1-4020-4399-4_192

Lay T, Kanamori H, Ammon CJ, Nettles M, Ward SN, Aster RC, Beck SL, Bilek SL, Brudzinski MR, Butler R, Deshon HR, Ekström G, Satake K, Sipkin S (2005) The great Sumatra-Andaman earthquake of 26 December 2004. Science 308(5725):1127–1133. https://doi.org/10.1126/science.1112250

Lindell MK, Lu JC, Prater CS (2005) Household decision making and evacuation in response to hurricane lili. Nat Hazards Rev 6(4):171–179. https://doi.org/10.1061/(ASCE)1527-6988(2005)6:4(171)

Lindell MK, Murray-Tuite P, Wolshon B, Baker EJ (2018) Large-scale evacuation: the analysis, modeling, and management of emergency relocation from hazardous areas (1st Edition). CRC Press, Cambridge. https://doi.org/10.4324/9781315119045

Lipa B, Barrick D, Isaacson J (2019) Evaluating HF coastal radar site performance for Tsunami warning. Remote Sens. https://doi.org/10.3390/rs11232773

Liu PLF, Woo SB, Cho YS (1998) Computer program for tsunami propagation and inundation. Cornell University, New York, p 25

Mansinha L, Smylie DE (1971) The displacement fields of inclined faults. Bull Seismol Soc Am. https://doi.org/10.1785/BSSA0610051433
Mas E, Suppasri A, Imamura F, Koshimura S (2012) Agent-based simulation of the 2011 Great East Japan earthquake/tsunami evacuation: an integrated model of tsunami inundation and evacuation. J Nat Disaster Sci 34(1):41–57. https://doi.org/10.2328/jnds.34.41
Meltzner AJ, Sieh K, Abrams M, Agnew DC, Hudnut KW, Avouac JP, Natawidjaja DH (2006) Uplift and subsidence associated with the great Aceh-Andaman earthquake of 2004. J Geophys Res Solid Earth. https://doi.org/10.1029/2005JB003891
Monecke K, Finger W, Klarer D, Kongko W, McAdoo BG, Moore AL, Sudrajat SU (2008) A 1000-year sediment record of tsunami recurrence in northern Sumatra. Nature 455(7217):1232–1234. https://doi.org/10.1038/nature07374
Muhari A, Imamura F, Suppasri A, Mas E (2012) Tsunami arrival time characteristics of the 2011 East Japan Tsunami obtained from eyewitness accounts, evidence and numerical simulation. J Nat Disaster Sci 34(1):91–104. https://doi.org/10.2328/jnds.34.91
Murotani S, Iwai M, Satake K, Shevchenko G, Loskutov A (2015) Tsunami forerunner of the 2011 Tohoku earthquake observed in the sea of Japan. Pure App Geophys 172(3–4):683–697. https://doi.org/10.1007/s00024-014-1006-5
Natawidjaja DH, Sieh K, Chlieh M, Galetzka J, Suwargadi BW, Cheng H, Edwards RL, Avouac JP, Ward SN (2006) Source parameters of the great Sumatran megathrust earthquakes of 1797 and 1833 inferred from coral microatolls. J Geophys Res Solid Earth. https://doi.org/10.1029/2005JB004025
National research council (2011) Tsunami Warning and Preparedness: An Assessment of the U.S. Tsunami Program and the Nation's Preparedness Efforts. The National Academies Press. https://doi.org/10.17226/12628
Newcomb KR, McCann WR (1987) Newcomb & McCann 1987. J Geophys Res 92(11):421–439. https://doi.org/10.1029/JB092iB01p00421
Nurendyastuti AK, Dinata MMM, Mitayani A, Purnama MR, Adityawan MB, Farid M, Kuntoro AA, Widyaningtias (2022) Tsunami early warning system based on maritime wireless communication. J. Civil Eng. Forum 8(2):115–124. https://doi.org/10.22146/jcef.2878
Okada Y (1985) Surface deformation due to shear and tensile faults in a half-space. Bull Seismol Soc Am 75(4):1135–1154. https://doi.org/10.1785/BSSA0750041135
Oktari RS, Munadi K, Ridha M (2014) Effectiveness of dissemination and communication element of tsunami early warning system in Aceh. Procedia Econ Financ 18:136–142. https://doi.org/10.1016/s2212-5671(14)00923-x
Park H, Cox DT (2016) Probabilistic assessment of near-field tsunami hazards: inundation depth, velocity, momentum flux, arrival time, and duration applied to Seaside. Oregon Coast Eng 117:79–96. https://doi.org/10.1016/j.coastaleng.2016.07.011
Péroche M, Leone F, Gutton R (2014) An accessibility graph-based model to optimize tsunami evacuation sites and routes in Martinique. France Adv Geosci 38:1–8. https://doi.org/10.5194/adgeo-38-1-2014
PusGen (2017) Peta Sumber dan Bahaya Gempa Indonesia Tahun 2017. Pusat Studi Gempa Nasional (Indonesia)
Ren Z, Liu H, Zhao X, Wang B, An C (2019) Effect of kinematic fault rupture process on tsunami propagation. Ocean Eng 181:43–58. https://doi.org/10.1016/j.oceaneng.2019.03.045
Rubin CM, Horton BP, Sieh K, Pilarczyk JE, Daly P, Ismail N, Parnell AC (2017) Highly variable recurrence of tsunamis in the 7400 years before the 2004 Indian Ocean tsunami. Nat Commun. https://doi.org/10.1038/ncomms16019
Satake K (1988) Effects of bathymetry on tsunami propagation: application of ray tracing to tsunamis. Pure Appl Geophys 126(1):27–36. https://doi.org/10.1007/BF00876912
Satake K, Kanamori H (1991) Use of tsunami waveforms for earthquake source study. Nat Hazards 4(2):193–208. https://doi.org/10.1007/BF00162787
Shen Y, Whittaker CN, Lane EM, Power W, Melville BW (2022) Interference effect on tsunami generation by segmented seafloor deformations. Ocean Eng. https://doi.org/10.1016/j.oceaneng.2021.110244
Shuto N, Matsutomi H (1995) Field survey of the 1993 Hokkaido Nansei-Oki earthquake tsunami. Pure Appl Geophys 144(3):649–663. https://doi.org/10.1007/BF00874388
Sufri S, Dwirahmadi F, Phung D, Rutherford S (2020) Progress in the early warning system in Aceh province, Indonesia since the 2004 earthquake-tsunami. Environ Hazards 19(5):463–487. https://doi.org/10.1080/17477891.2019.1653816
Syamsidik RTM, Kato S (2015) Development of accurate tsunami estimated times of arrival for tsunami-prone cities in Aceh, Indonesia. Int J Disaster Risk Reduct 14:403–410. https://doi.org/10.1016/j.ijdrr.2015.09.006

Synolakis C, Okal E, Bernard E (2005) The Megatsunami of December 26, 2004. The Bridge, Summer 2005. https://www.pmel.noaa.gov/pubs/PDF/syno2380/syno2380.pdf

Tim Kaji Cepat (2011) Evaluasi Sistem Peringatan Dini Tsunami pada Kejadian Gempabumi & Tsunami Aceh 11 April 2012. Laporan Awal Kaji Cepat Bersama, BMKG – BNPB – LIPI – BPPT – RISTEK - GIZ-IS PROTECTS - UNESCO-JTIC - UNDP - KKP - Tohoku University - TDMRC - Universitas Syiah Kuala - UNDP - DRRA Universitas Andalas - Universitas Bung Hatta - KOGAMI. https://www.gitews.org/tsunami-kit/en/E4/further_resources/case_study/Evaluasi%20Sistem%20Peringatan%20Dini%20Tsunami%20pada%20Kejadian%20Gempabumi%20&%20Tsunami%20Aceh%2011%20April%202012.pdf

Titov VV, Moore CW, Greenslade DJM, Pattiaratchi C, Badal R, Synolakis CE, Kânoğlu U (2011) A new tool for inundation modeling: community modeling interface for tsunamis (ComMIT). Pure Appl Geophys 168(11):2121–2131. https://doi.org/10.1007/s00024-011-0292-4

Titov VV, Gica E, Spillane MC (2008) Development of the Forecast Propagation Database for NOAA's Short-term Inundation Forecast for Tsunamis (SIFT). https://repository.library.noaa.gov/view/noaa/11079

Tsuji Y, Tanioka Y, Matsutomi H, Nishimura Y, Kamataki T, Murakami Y, Sakakiyama T, Moore A, Gelfenbaum G, Nugroho S, Waluyo B, Sukanta I, Triyono R, Namegaya Y (2006) Damage and height distribution of sumatra earthquake-tsunami of December 26, 2004, in Banda Aceh City and its Environs. J Disaster Res 1(1):103–115. https://doi.org/10.20965/jdr.2006.p0103

Tursina S, Kato S, Afifuddin M (2021) Coupling sea-level rise with tsunamis: projected adverse impact of future tsunamis on Banda Aceh city, Indonesia. Int J Disaster Risk Reduct. https://doi.org/10.1016/j.ijdrr.2021.102084

United Nations Inter-Agency Secretariat of the International Strategy for Disaster Reduction (UN/ISDR) (2006) Global Survey of Early Warning Systems: An assessment of capacities, gaps and opportunities towards building a comprehensive global early warning system for all natural hazards. https://www.unisdr.org/2006/ppew/info-resources/ewc3/Global-Survey-of-Early-Warning-Systems.pdf

Wang D, Mori J, Uchide T (2012) Supershear rupture on multiple faults for the Mw 8.6 off Northern Sumatra, Indonesia earthquake of April 11, 2012. Geophys Res Lett. https://doi.org/10.1029/2012GL053622

Wang H, Mostafizi A, Cramer LA, Cox D, Park H (2016) An agent-based model of a multimodal near-field tsunami evacuation: Decision-making and life safety. Trans Res Part C Emerg Technol 64:86–100. https://doi.org/10.1016/j.trc.2015.11.010

Wang X (2009) User Manual for COMCOT Version 1.7 (first draft). http://ceeserver.cee.cornell.edu/pllgroup/comcot_down.htm.

Weller O, Lange D, Tilmann F, Natawidjaja D, Rietbrock A, Collings R, Gregory L (2012) The structure of the Sumatran Fault revealed by local seismicity. Geophys Res Lett. https://doi.org/10.1029/2011GL050440

Wells DL, Coppersmith KJ (1994) New empirical relationships among magnitude, rupture length, rupture width, rupture area, and surface displacement. Bull Seismol Soc Am 84(4):974–1002

Wood N, Jones J, Peters J, Richards K (2018) Pedestrian evacuation modeling to reduce vehicle use for distant tsunami evacuations in Hawai'i. Int J Disaster Risk Reduct 28:271–283. https://doi.org/10.1016/J.IJDRR.2018.03.009

Authors and Affiliations

Benazir[1] · Rina Suryani Oktari[2]

✉ Benazir
benazir@ugm.ac.id

[1] Department of Civil and Environmental Engineering, Faculty of Engineering, Universitas Gadjah Mada, Jl. Grafika, Kampus No.2, Yogyakarta, Indonesia

[2] Department of Family Medicine, Faculty of Medicine Graduate Program in Disaster Science, Tsunami & Disaster Mitigation Research Center (TDMRC), Universitas Syiah Kuala, Darussalam, Banda Aceh, Indonesia